Low contrast buried waveguides index profile reconstruction method considering the evanescent field

2015 J. Opt. 17 085801

(http://iopscience.iop.org/2040-8986/17/8/085801)

IOP Publishing Journal of Optics
J. Opt. 17 (2015) 085801 (7pp) doi:10.1088/2040-8978/17/8/085801

Low contrast buried waveguides index profile reconstruction method considering the evanescent field

Demian A Biasetti, Matías R Tejerina and Gustavo A Torchia

Centro de Investigaciones Ópticas, CONICET La Plata–CICBA, Camino Centenario y 506 s/n, M.B Gonnet (1897), Pcia. de Buenos Aires, Argentine Republic

E-mail: gustavot@ciop.unlp.edu.ar

Received 30 March 2015, revised 20 May 2015
Accepted for publication 27 May 2015
Published 20 July 2015

Abstract

In this work we present a new approach related to the profile reconstruction of graded-index waveguides, based on the inversion of the Helmholtz equation for transversal electric propagation modes from measuring the near field. We used the scalar approximation, but we also consider the evanescent field as key experimental data to be acquired and analyzed. From this, it is possible to obtain a better fitting of the real low-contrast waveguide index profile and get more important information, allowing us to determine at the same time the effective index and the shape of the guidance cross section. Compared with experimental data, it could be possible, in a self-consistent way, to enhance the accuracy of the retrieval information corresponding to the transversal shape of these kinds of waveguides. This procedure also allows us to obtain an effective and absolute refractive index profile instead of the relative determinations that are usually reported in the literature.

Keywords: effective index, waveguides, femtosecond laser writing

1. Introduction

Since the commercial impact of the amplified femtosecond (fs) laser systems at the end of the 20th century, many researchers around the world have studied the ultra-short laser interaction with optical materials. From these studies and their main applications, suitable optical circuits and waveguiding structures have been performed in either active or passive materials [1–5]. In order to improve and control the resultant guiding structures, a deeper knowledge of their refractive index profile is needed.

As is well known, many complex processes, which include nonlinear absorption (multi-photon, avalanche, and tunnel), Coulomb explosion, shock wave propagation, etc, among other phenomena, are activated during/after the interaction of fs laser pulses and matter. Some works based on computational simulations plus empirical methods have been used to report the final waveguide profile [6–9]. In these papers, some authors have considered a mechanical expansion in the region where the fs pulses write the optical breakdown track inside the material [10, 11].

To quantify the refractive index profile for the femtosecond written structures, standard methods can be used. There is a substantial amount of work dealing with the reconstruction of the waveguide index profile. Many studies are based on the inversion of the scalar wave equation for transversal electric (TE) modes and the intensity measured from the near field [9, 12–16]. However, some simplifications made in those works allow only a qualitative description of the cross section of the refractive index profile.

In this work, we also used the mentioned scalar equation, but we have additionally considered the evanescent field as key experimental data. From acquiring and analyzing the evanescent field, it is possible to obtain a better fitting of the real low- contrast waveguide index profile and get more important information to determine simultaneously the effective index and the shape of the cross-guidance section.

In particular, in this work we have investigated waveguides fabricated by the direct femtosecond laser writing [17] technique in fused silica samples.

As is well known, in order to achieve a good fitting of the waveguide's shape, a high spatial and intensity resolution of

the near field is necessary. We have therefore considered the experimental conditions in order to minimize the error in the numerical determination of the refractive index profile.

2. Theoretical framework and remarks

Cross-section profile reconstruction is usually based on the inversion of the scalar wave equation (1), where n(x, y) is the refraction index profile of the buried waveguide analyzed.

$$n(x, y) = \left[\frac{\beta^2}{k_0^2} - \frac{\nabla_T^2 E_y(x, y)}{k_0^2 E_y(x, y)} \right]^{1/2}. \quad (1)$$

In (1), $E_y(x, y)$ is the transversal field component of a TE fundamental mode, ∇^2_T is the transversal Laplacian operator, k_0 is the wavenumber corresponding to the free propagation wavelength, and β is the propagation constant (related with effective index $N_{eff} = \beta/k_0$). The value of the effective index ranges between the substrate index and the maximum index of the waveguide, and it can reach different values corresponding to the different propagation modes ($n_s < N_{eff} < n_{max}$).

For our analysis, it is suitable to rewrite (1) as (2):

$$n(x, y)^2 - N_{eff}^2 = -\frac{\nabla_T^2 E_y(x, y)}{k_0^2 E_y(x, y)} = 2n_s z(x, y). \quad (2)$$

For convenience, we defined the z-function $z(x, y)$ in this way. In this equation, N_{eff} is taken into account, unlike in previous works where N_{eff} is assumed to be equal to the substrate refractive index (n_s). We think that this point is a weak assumption that is widely used in the published works. This means an uncertainty in the absolute determination of the refractive index profile due the unknown constant N_{eff}. From the literature, this constant is considered zero.

An important fact observed from (2) is that the contour lines, where the Laplacian vanishes, occur when the real part of the refractive index becomes equal to the value of the effective index N_{eff}. Usually, in one-dimensional waveguide reconstruction methods, such as the inverse Wentzel–Kramers–Brillouin method [18, 19], it is considered that these are special physical points where the value of the refractive index equals that of the effective refractive index. These places are known as the 'turning points' [9, 20]. Analogously, in two-dimensional problems, there is a continuous set of turning curves that satisfy the following equation:

$$\nabla_T^2 E_y(x_t, y_t) = 0 \quad (3)$$

where (x_t, x_t) are the turning points in the cross section of the waveguide, where (4) is also satisfied.

$$n(x_t, y_t) = N_{eff} \quad (4)$$

$$n(x, y) = n_s + \Delta n(x, y) \quad (5)$$

$$z(x, y) \approx \Delta n(x, y) - \Delta N \quad (6)$$

Furthermore, we describe the refractive index profile by (5) and the effective refractive index by $N_{eff} = \Delta N + n_s$. In this expression, the new scalar value ΔN is defined.

Then, replacing the expressions of N_{eff} and $n(x, y)$ into (2), we obtain (6). In this procedure, the low-contrast index condition ($\Delta n(x, y) \ll n_s$), is assumed.

The z-function has an asymptotic convergence towards the $-\Delta N$ constant in the infinitum (i.e., in the substrate). This is because of the waveguide definition. The refractive index in the infinitum must be equal to the substrate refractive index n_s,

Or, equivalently,

$$\Delta n(x, y)|_{\infty} = 0.$$

Additionally, the maximum Δn_0 of the contrast index function $\Delta n(x, y)$ will be reached at (x_0, y_0), where the z-function satisfies the condition:

$$\vec{\nabla} z(x, y)\Big|_{(x_0, y_0)} = 0. \quad (7)$$

So, we have defined two important points in the index profile: the 'turning point' and the 'maxima point' (x_0, y_0). Then, it is possible to use these to attempt some analytical function that approaches the z-function.

3. Reconstruction method

3.1. Experimental setup and optical resolution

We fabricated a 'simple-track' waveguide inside a fused silica sample of $20 \times 20 \times 5$ mm^3. This guiding structure was fabricated using a chirped pulse amplificaation system that can deliver a 120 fs pulse width at 800 nm of peak wavelength, 1 kHz repetition rate, and up to 1 mJ per pulse. The writing parameters used in this work were: 30 μm/s translation speed and 2 μJ of energy per pulse. The details of the waveguide fabrication procedure can be found in [17]. These parameters induced, in fused silica, an increment of refractive index adjacently to the focal volume, wherewith we fabricate type II waveguides [4].

We measured the fundamental mode near field of the fabricated waveguide structure by using the 'end fire' method [15]. With these experimental data, we computed the numerical z-function. Prior to this computing, the near-field data were filtered, taking into account a correct Butterworth (BW) filter according to [12–15]. The optical resolution determines the spatial resolution of the image acquired by the charge coupled device (CCD), and thus the cut-off spatial frequency used in the filtering process. Therefore, it is necessary to take into account the diffraction limit and the optical zoom conducted in the experiment.

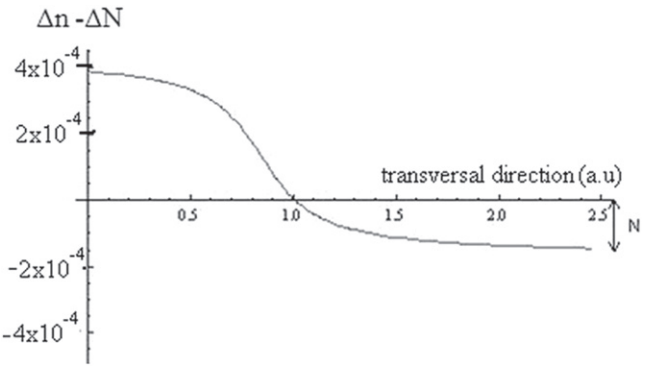

Figure 1. Qualitative transversal profile of z-function.

3.2. Fitting procedure

In this section, we present firstly the requirements that must be taken into account to attempt any kind of fitting between the experimental data and the analytical function and, secondly, a new algorithm to solve the unknown refractive index profile.

Considering (6) and (7), it is easy to show the z-function to be physically a refractive index field that must satisfy the following conditions:

(i) $\lim_{(x,y)\to\pm\infty} z(x, y) = -\Delta N = \text{constant} < 0$
(ii) z has a maximum positive at some point (x_0, y_0)
(iii) $z(x_0, y_0) = n(x_0, y_0) - N_{eff} > 0$

Figure 1 illustrates qualitatively these conditions in any arbitrary transversal direction.

Also, we expect that contour lines corresponding to the z-function are close due to continuity on the refractive index variation, the substrate index being the asymptotic value of this. These curves could be parametric curves, similar to ellipses.

The high-precision measurement of the evanescent field, corresponding to the coupled electrical transversal modes, could allow computation of the z-function beyond the turning points and, therefore, evaluation of the refractive index field too. In this work, we analyze two possible fittings for the so-called 'simple' and 'double track' waveguide structures fabricated with the ultra-short laser writing technique.

3.2.1. Simple track. In this case, we can propose $\Delta n(x, y) = \Delta n_0 h(x, y)$ where $h(x, y)$ is the function that will be fitted, which is illustrated by a colour map in figure 2 near the track (dark zone). Now, considering two perpendicular lines crossing each other in the origin, one horizontal and the other vertical. For convenience, the coordinate origin can be set at maxima point, which has been defined by (7) in section 2, so that $\Delta n_0 = \Delta n(0, 0)$ or, equivalently, $h(0, 0) = 1$. The 'maxima point' must be obtained by numerical algorithm from processed experimental data as well as the turning curve by (3).

Then, these lines intersect the turning curve at two points each one, as shown in figure 3. Both the vertical and the horizontal lines intersect the contour lines defined by (3) at (0, yt) and (xt, 0), respectively,as shown in figure 3(b).

So, we have for the horizontal line:

$$z(x, 0) \approx \Delta n_0\left[h(x, 0) - h\left(x_t, 0\right)\right] = \Delta n_0 h_1(x) - N_{eff} + n_s \quad (8a)$$

where $h_1(x) = h(x, 0)$. And for the vertical line:

$$z(0, y) \approx \Delta n_0\left[h(0, y) - h\left(0, y_t\right)\right] = \Delta n_0 h_2(y) - N_{eff} + n_s \quad (8b)$$

where $h_2(y) = h(0, y)$.

In order to fit the parameters involved in the proposed functions h_1 and h_2, the turning points x_t, y_t must be passed as fixed values from the experimental data. Finally, the fitting of h_1 and h_2 provide us N_{eff} and Δn_0.

In this case, the consistency of fitting is determined by the degree of matching between the independent N_{eff} values obtained after fitting expressions (8a) and (8b) for the horizontal and vertical axis, respectively.

Also, it is possible to compute a mean value of the effective index obtained from a series of vertical and horizontal fittings, as described above. This mean value should have a standard deviation similar to the numerical propagation error of the refractive index to be acceptable. The fitting must be iterated until this condition is reached.

Finally, simulation software must be used to test the results, comparing the simulated field mode obtained by the fitted profile with the experimental filtered field mode as in [9].

3.2.2. Double track. In the double-track approach, because of the focal volume geometry in the femtosecond laser interaction zone [16], we can expect some symmetry in the resultant refractive index profile. Thus, we can propose the following expression, corresponding to the refractive index:

$$\Delta n(x, y) = \Delta n_0 f(x) g(y) \quad (9)$$

where $f(x)$ and $g(x)$ are analytical functions normalized. Figure 2 shows a cross section corresponding to a simulated half part of the waveguide structure.

So by using expressions (4), (5), and (6), we arrive at

$$z(x, y) \approx \Delta n_0\left[f(x)g(y) - f(x_t)g(y_t)\right]$$

For convenience, this point can be chosen as the coordinates origin, so that $\Delta n_0 = \Delta n(0, 0)$ or, equivalently, $f(0)g(0) = 1$ in agreement with (9). Moreover, it is free the choice $f(0) = g(0) = 1$. Then, taking into account this prescription, and considering two perpendicular lines crossing each other in the origin (maxima point), one horizontal and the other vertical, we can attempt an independent fitting for both the $f(x)$ and $g(y)$ functions in (9). These lines go across the contour turning curve determined by (3). This cross was illustrated in figure 3 for the simple track. Hence, for the

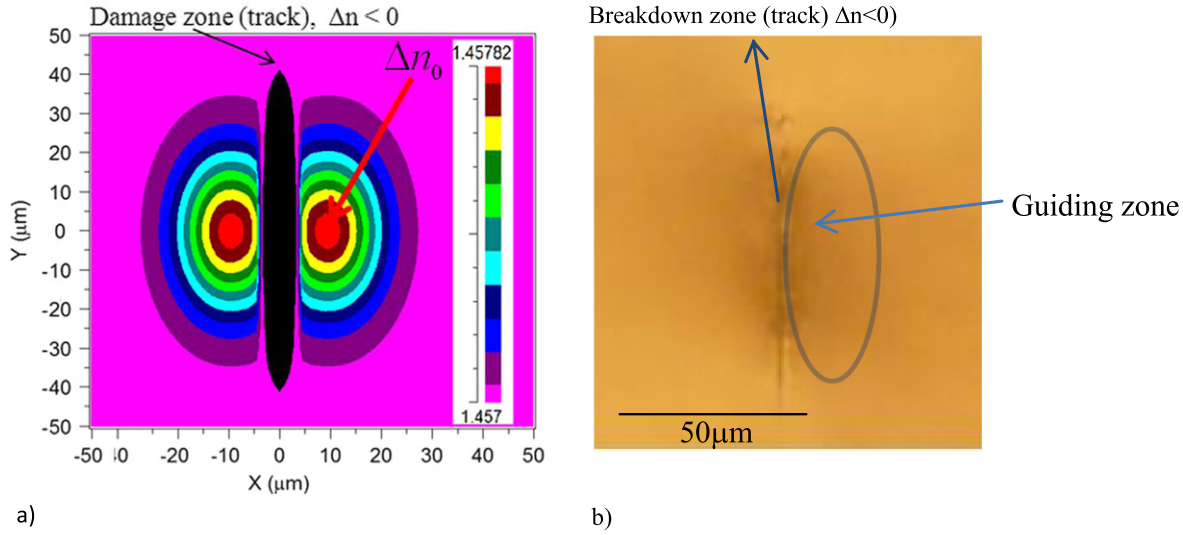

Figure 2. Simple track waveguide is shown. (a) Colour map of a simulated cross-index profile of simple-track waveguide type II structure. (b) Transmission optical microscopy of simple-track cross section in fused silica. It is possible to appreciate the filament or track of optical breakdown and asides it (to the right and to the left) a diffused zone where $\Delta n > 0$. Laser was focused from the top.

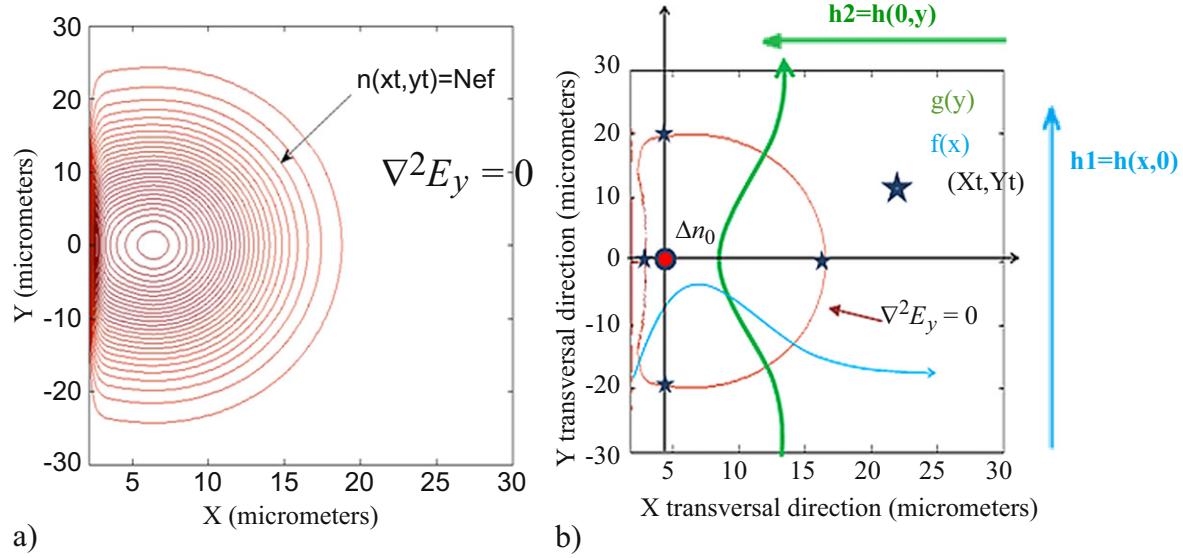

Figure 3. (a) Contour line where the Laplacian of field E_y vanishes. (b) Simulated turning curve where $n = N_{\text{eff}}$, as well as qualitative crossing, pass this contour turning line.

horizontal line we have:

$$z(x, 0) \approx \Delta n_0 \left[f(x) g(0) - f(x_t) g(y_t) \right] = A f(x) - N_{eff} + n_s \tag{10}$$

where $A = \Delta n_0\, g(0)$. Then, fitting the A and N_{eff} parameters and those involved in the proposed $f(x)$, by using numerical data $z(x, 0)$, and since $f(0)g(0) = 1$, it is possible to calculate Δn_0 by using equation (9) and obtaining the horizontal profile as follows:

$$\Delta n(x, 0) = A f(x) = \Delta n_0 f(x) g(0).$$

Proceeding in a similar way with the vertical line, we obtain an analogous equation:

$$\Delta n(0, y) = B g(y) = \Delta n_0 f(0) g(y).$$

The consistency of the method will be established by matching the N_{eff} with $f(x_t)g(0)$ after fitting the parameters[1]. Also, consistency is defined by the agreement between both the horizontal and vertical fit.

[1] Where $f(x_t)$ is the analytical expression of $f(x)$ obtained after fit valued in x_t.

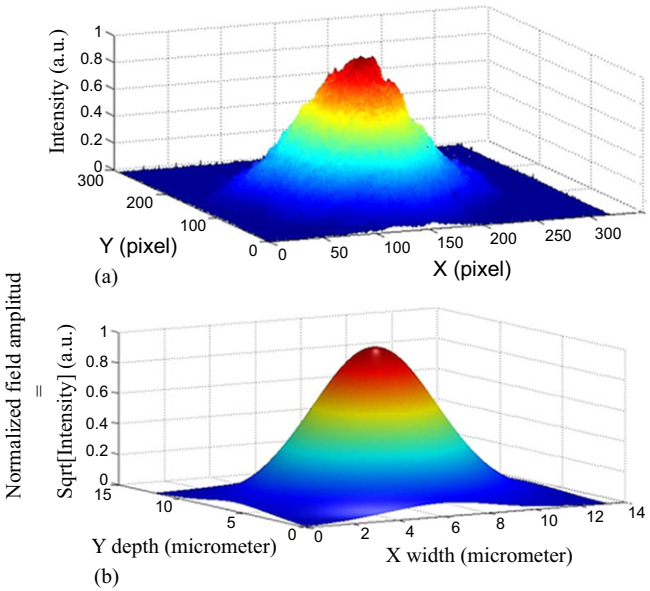

Figure 4 (a). Waveguide TE_{00} experimental CCD-acquired mode without filtering. (b) Waveguide TE_{00} mode filtered and spatially scaled.

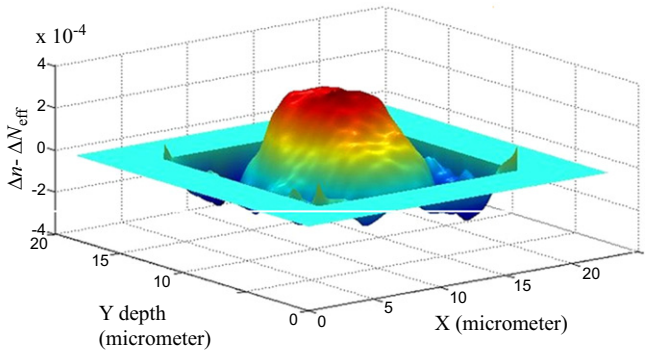

Figure 5. *Z*-function obtained numerically from experimental data.

4. Analysis and results

Figure 4 shows the experimental mode coupled to the waveguide by an 'end-fire' system, where the intensity is collected through a 10-bit CCD, $7 \times 7\,\mu m^2$ pixel size, and 56 Db dynamical range. The *z*-function was numerically obtained, considering the approximation of phase invariance of the mode along the propagation direction, once the mode was collected from the waveguide end-face, by focusing a 40X microscopy objective. Thus, considering $E(x, y) = I(x, y)^{1/2}$, the z-function is shown in figure 5 after processing the numerical matrix data with a BW filter, according to [12] and [15]. Also, it can be possible to apply the algorithm proposed in [21].

Also, we plot in figure 6 the contour of the experimental field amplitude Laplacian, according to (3). Finally, finding the maxima point of the *z*-function, we plot both the *yz* and *xz* profiles crossing that point. Figures 7(a) and (b) show the polynomial fitting. The outside limit of these curves shows a flatness behavior followed by the undesired growing tail, which is a consequence of numerical apodization. The

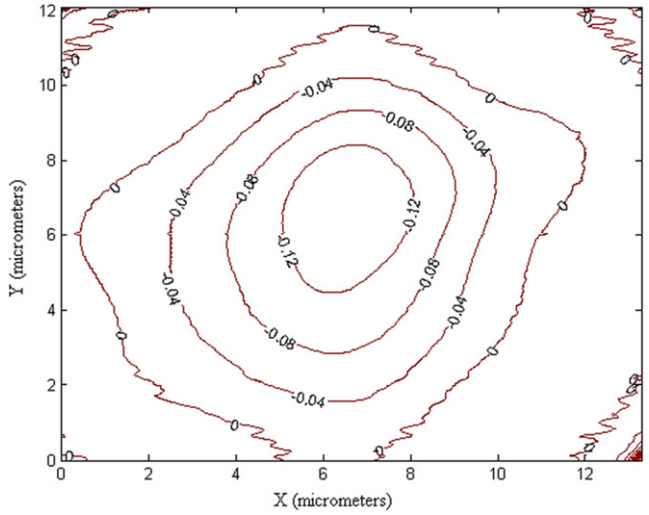

Figure 6. Level curves of *z*-function. The zero value corresponds to the turning curve, where the refractive index is equal to the effective index.

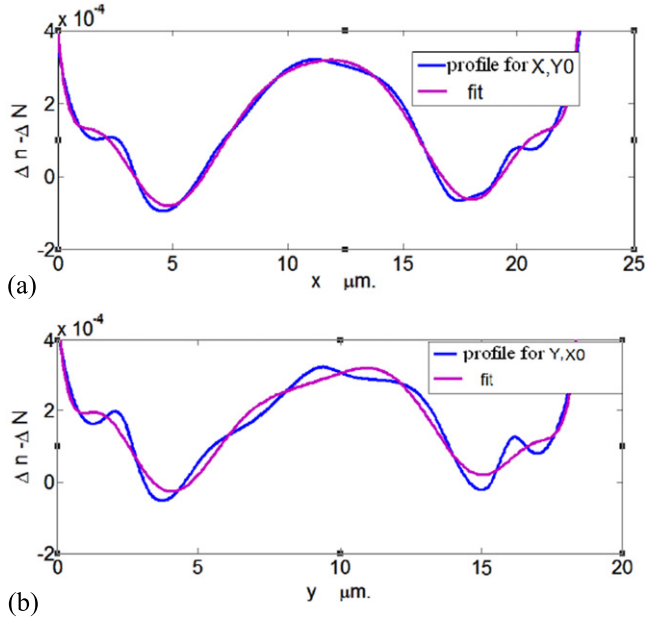

Figure 7. Transversal *z*-function profile of horizontal (a) and vertical lines (b).

difference between the flatness value and local minima gives us the ΔN value.

4.1. Error analysis

Previous works have already pointed out the error amplification due to the Laplacian operator [12–14]. In [22] is proposed an experimental method in order to minimize that error by measuring first- and second-order derivatives of modal intensity. However, the numerical calculus of the Laplacian discrete field, and hence the *z*-function, implies a finite error in the calculus procedure. These error contributions are the quantization error as well as the spatial resolution. The former is considered where the signal-to-noise ratio (SNR) remains

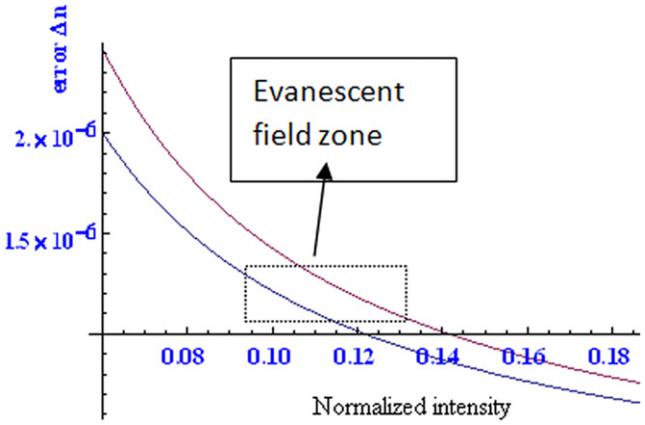

Figure 8. Contributions to experimental error for Δn as a function of the intensity in an arbitrary direction. This is equivalent to fixing a pixel and varying the normalized intensity to unity.

high enough, and the latter is determined by optical resolution r where the condition $P/M < r$ must be satisfied. P is the pixel width and M the optical zoom. The resolution r is calculated by the Rayleigh criterion for a coherent light source.

While quantization error can be reduced by setting a suitable gain in the CCD system, keeping the SNR high enough, spatial resolution can be reduced by the numerical aperture of the optical lens employed.

Figure 8 shows both contributions of errors as functions of the normalized intensity of the waveguide mode. Considering the contour line given by equation (3), we estimated the ratio of the field to the maximum. Thus, figure 8 shows the window where the refractive index is equal to the effective index, which is used to fit the analytical profile in a self-consistent way. The error was parameterized with the CCD gain, the pixel error size, and the slope of field, which appears when applying finite differences to the right term of (2). The latter was established, taking an upper limit according to experimental data, and finally used in the error propagation equation of the right term of (2). Figure 8 shows the overall error using the mentioned parameters, which provide an upper limit, ensuring an acceptable value for the reconstructed refractive index profile.

5. Discussion

We put forward a self-consistent method of refractive index profile reconstruction in low-contrast waveguide structures without omitting the absolute value of the effective index, which is passed over in the literature. We question this weak point, because it is possible to resolve very low-value differences between the effective index and index substrate, keeping the measurement parameters, providing a 10% or lower error in the evanescent field zone.

In this way, the determination of the absolute effective index improves our knowledge of the absolute refractive index modification at a deeper level. The method also allows determination of the cross-section shape of the waveguides, which can be useful for many investigative purposes, such as correlations between micro-machining parameters and refractive index modification, or between coupling zones and insertion losses. These purposes are directly related to the evanescent field. Despite the impossibility of finding smooth parametric curves like ellipses to be matched with those calculated from equation (3), the study presented in this paper provides a starting point for a deeper knowledge corresponding to induced modification in the refractive index by femtosecond laser in several optical materials.

In this work, we found the fitting function constraints and, in consequence, we left open its election. It should be pointed out that a couple of functions must probably be combined in order to verify the required conditions mentioned above.

Although we described fitting in waveguides with some symmetries, it is possible to expand the method for arbitrary profiles without factorizing the functions. In these general cases, one must previously fit the mode field, taking into account the required conditions (section 2.2), then executing z-function calculus with the analytical field function obtained. Finally, in this case, we observed that Gaussian functions are not suitable functions for the modal field, because if it were the case, the z-function could not strictly satisfy condition (i) in section 2.2.

6. Conclusion

From this work it is possible to achieve a deep knowledge of the refractive index profile in low-contrast waveguides. We demonstrate that the possibility of near-field measurement with a low experimental error in the field tail zone (evanescent field) leads to a more complete description of cross-section waveguides. The method proposed for the refractive index reconstruction provides an absolute value of the refractive index as well as an effective index of the fundamental mode and waveguide shape. In spite of this, we do not offer possible fitting functions, corresponding to the refractive index; we established a hypothesis about the symmetries of which we took advantage to simplify the fitting process. The results achieved are capable to provide us intrinsic losses due to the evanescent field. So, these are related with optical guiding performance and coupling coefficients, which are very important in considering technological applications for these kinds of waveguiding structures.

Acknowledgments

The authors wish to thank Dr Alberto Lencina for provide the 10-bit CCD camera to carry out the experiment. The authors also would like to thank Fabian Videla for the fruitful discussion about the assumptions proposed for the reconstruction method development.

References

[1] Della Valle G, Osellame R and Laporta P 2009 Micromachining of photonic devices by femtosecond laser pulses *J. Opt. A: Pure Appl. Opt.* **11** 013001

[2] Ams M, Marshall G D, Dekker P, Piper J A and Withford M J 2009 Ultrafast laser written active devices *Laser Photonics Rev.* **3** 535–44

[3] Osellame R, Cerullo G and Ramponi R (ed) 2012 Femtosecond laser micromachining *Topics in Applied Physics* (Berlin: Springer)

[4] Chen F and de Aldana J R V 2013 Optical waveguides in crystalline dielectric materials produced by femtosecond-laser micromachining *Laser Photonics Rev.* **8** 251–75

[5] Calmano T and Muller S 2015 Crystalline waveguide lasers in the visible and near-infrared spectral range *IEEE J. Select. Topics Quantum Electron.* **21** 401–13

[6] Oberson P, Gisin B, Huttner B and Gisin N 1998 Refracted near-field measurements of refractive index and geometry of silica-on-silicon integrated optical waveguides *Appl. Opt.* **37** 7268

[7] Dong N, Martínez de Mendivil J, Cantelar E, Lifante G, Vázquez de Aldana J, Torchia G A, Chen F and Jaque D 2011 Self-frequency-doubling of ultrafast laser inscribed neodymium doped yttrium aluminum borate waveguides *Appl. Phys. Lett.* **98** 181103

[8] Ródenas A, Maestro L M, Ramírez M O, Torchia G A, Roso L, Chen F and Jaque D 2009 Anisotropic lattice changes in femtosecond laser inscribed Nd[sup 3+]:MgO:LiNbO[sub 3] optical waveguides *J. Appl. Phys.* **106** 013110

[9] Biasetti D, Neyra E, Vázquez de Aldana J R, Roso L and Torchia G A 2013 Buried waveguides in Nd:YLF crystals obtained by femtosecond laser writing under double line approach *Appl. Phys.* A **110** 595–9

[10] Burghoff J, Nolte S and Tünnermann A 2007 Origins of waveguiding in femtosecond laser-structured $LiNbO_3$ *Appl. Phys.*A **89** 127–32

[11] Tejerina M R, Jaque D and Torchia G A 2014 A 2D μ-Raman analysis of low repetition rate femto-waveguides in lithium niobate by using a finite element model *Opt. Mater.* **36** 936–40

[12] Von Bibra M L and Roberts A 1997 Refractive index reconstruction of graded-index buried channel waveguides from their mode intensities *J. Lightwave Technol.* **15** 1695–9

[13] Mansour I and Caccavale F 1996 An improved procedure to calculate the refractive index profile from the measured near-field intensity *J. Lightwave Technol.* **14** 423–8

[14] Ganguly P, Sones C L, Youngjin Ying H, Steigerwald K, Buse E, Soergel R W, Eason and Mailis S 2009 Determination of refractive indices from the mode profiles of UV-written channel waveguides in LiNb03-crystals for optimization of writing conditions *J. Lightwave Technol.* **27** 3490–7

[15] Ghosh T, Samanta B, Jana P C and Ganguly P 2012 Determination of refractive index profile and mode index from the measured mode profile of single-mode LiNbO3-diffused waveguides *Fiber Integr. Opt.* **31** 1–10

[16] Lin J-H, Chen C-K and Lin Y-J 2002 An improved inverse method for refractive index reconstruction of ion-exchanged waveguides *J. Opt. Commun.* **23** 29–34

[17] Gattass R R and Mazur E 2008 Femtosecond laser micromachining in transparent materials *Nature Photon.* **2** 219

[18] Marcuse D 1973 TE modes of graded-index slab waveguides *IEEE J. Quantum Electron.* **9** 1000–6

[19] Chiang K 1985 Construction of refractive-index profiles of planar dielectric waveguides from the distribution of effective indexes *J. Lightwave Technol.* **3** 385–91

[20] Lifante G 2005 *Integrated Photonics: Fundamentals* (New York: Wiley) p 80

[21] Barai S and Sharma A 2009 Inverse algorithm with built-in spatial filter to obtain the 2D refractive index profile of optical waveguides from the propagating mode near-field profile *J. Lightwave Technol.* **27** 1514–21

[22] Tsai W-S, Ting S-Y and Wei P-K 2012 Refractive index profiling of an optical waveguide from the determination of the effective index with measured differential fields *Opt. Express* **20** 26766